

Origin of pancreatic ductal adenocarcinoma from atypical flat lesions: a comparative study in transgenic mice and human tissues.

Running title: Precursor lesions in pancreatic ductal adenocarcinoma

Michaela Aichler^{1*}, Christopher Seiler^{2*}, Monica Tost^{1*}, Jens Siveke³, Pawel K. Mazur^{3†}, Patricia Da Silva-Buttkus¹, Detlef K. Bartsch⁴, Peter Langer⁴, Sara Chiblak⁵, Anna Dürr⁶, Heinz Höfler⁶, Günter Klöppel⁶, Karin Müller-Decker⁵, Markus Brielmeier⁷, Irene Esposito^{1,6}

¹Institute of Pathology, Helmholtz Zentrum München, Neuherberg, Germany

²Institute of Pathology, University of Heidelberg, Heidelberg, Germany.

³Department of Internal Medicine, Klinikum Rechts der Isar, Technische Universität München, Munich, Germany

⁴Department of Surgery, Philipps-University, Marburg, Germany

⁵Core Facility Tumor Models, Deutsches Krebsforschungszentrum, Heidelberg, Germany

⁶Institute of Pathology, Technische Universität München, Munich, Germany

⁷Department of Comparative Medicine, Helmholtz Zentrum München, Neuherberg, Germany

*equal contribution

†Present address: Stanford University, Medical School, Department of Genetics, Stanford Stem Cell Biology and Regenerative Medicine Institute, Stanford, CA

The authors declare that there are no conflicts of interest

Corresponding author and address for reprint requests:

Irene Esposito, MD

Institute of Pathology

Technische Universität München

Ismaningerstr. 22

81675 Munich

Germany

Esposito@lrz.tum.de

Abstract

Pancreatic ductal adenocarcinoma (PDAC) and its precursor lesions, pancreatic intraepithelial neoplasia, (PanIN), display a ductal phenotype. However, there is evidence in genetically defined mouse models for PDAC harbouring a mutated *kras* under the control of a pancreas-specific promoter that ductal cancer might arise in the centroacinar-acinar region, possibly through a process of acinar-ductal metaplasia (ADM). In order to further elucidate this model of PDAC development, an extensive expression analysis and molecular characterization of the putative and already established (PanIN) precursor lesions was performed in the *Kras*^{G12D/+};*Ptf1a-Cre*^{ex1/+} mouse model and in human tissues, focusing on lineage markers, developmental pathways, cell cycle regulators, apomucins and stromal activation markers. The results of this study show that areas of ADM are very frequent in the murine and human pancreas and represent regions of increased proliferation of cells with precursor potential. Moreover, atypical flat lesions originating in areas of ADM are the most probable precursors of PDAC in the *Kras*^{G12D/+};*Ptf1a-cre*^{ex1/+} mice and similar lesions were also found in the pancreas of three patients with a strong family history of PDAC. In conclusion, PDAC development in *Kras*^{G12D/+};*Ptf1a-Cre*^{ex1/+} mice starts from ADM and a similar process might also take place in patients with a strong family history of PDAC.

Keywords: familial pancreatic cancer, PanIN, tubular complexes, precursor lesions, mouse model, *Kras*

Introduction

Identification of tumour precursors represents a basic strategy of secondary cancer prevention that allows the definition of screening programmes, which have been shown to dramatically improve the prognosis of common human neoplasms, such as colon and breast cancer. The key for the success of such screening strategies is the exact clinical, morphological and molecular characterization of the precursors and the development of rational, cost-effective methods for early detection and therapy. The prognosis of PDAC would be greatly affected by such screening strategies, since surgery in early stages still represents the only chance to achieve prolonged survival rates [1,2].

Pancreatic Intraepithelial Neoplasia (PanIN) has been identified as the most common precursor lesion of PDAC, this evidence being substantiated by molecular analysis and recently developed endogenous mouse models [3,4,5,6]. The molecular steps of PanIN progression to invasive PDAC have been defined as well. In particular, activating mutations of the protooncogene *Kras*, which are detected in 36%, 44%, and 87% of cancer associated PanIN1A, PanIN1B, and PanIN2-3, respectively, represent the earliest genetic change [7]. The relevance of *Kras* in pancreatic cancer progression has been further underscored by the development of engineered mouse models harbouring activating *kras* mutations in the endogenous locus under a pancreas-specific promoter, such as *pdx1* or *ptf1a*, which develop the full spectrum of the human disease, including lesions similar to human PanIN [6].

Accurate histopathological examination of the pancreas of patients with a strong family history of pancreatic cancer has confirmed the role of PanIN as precursors of human PDAC. In fact, multiple PanIN with different degrees of dysplasia have been

reported in patients with familial pancreatic cancer (FPC) undergoing prophylactic total pancreatectomy [8,9].

PanIN and other PDAC precursors, such as intraductal papillary-mucinous neoplasm (IPMN) and mucinous cystic neoplasm (MCN) display a ductal phenotype, thus indicating the pancreatic ducts as the site of origin of pancreatic cancer [10]. However, recent evidence emerging from mouse models and lineage tracing studies challenged the duct system as the only site from where PDAC originates. It is suggested that PDAC develops in the centroacinar-acinar compartment (CAAC) through a process of acinar-ductal metaplasia (ADM) or through the expansion of the centroacinar cells accompanied by apoptosis of the acinar cells [11-13]. Ductular structures characterized by mucin production (mucinous metaplastic lesions, MML) are frequently observed within the acinar parenchyma of transgenic mouse models of PDAC and could represent an intermediate stage preceding the development of mouse PanIN (mPanIN) [14]. In a previous study, we analyzed the incidence and distribution of such ductular structures with and without mucinous metaplasia, which we respectively called mucinous tubular complexes (MTC) or tubular complexes (TC), in a large collection of human specimens [15]. We were able to demonstrate that TC and MTC are common lesions in the human pancreas, and that the expression of acinar markers, like trypsin, is retained in advanced PanIN lesions, an observation that has been confirmed by others [16]. These findings led us to propose a model for the origin of pancreatic cancer in the periphery of the ductal system, with a strong parallelism to the origin of ductal breast cancer in the terminal ductular-lobular unit (TDLU) of the mammary gland [17].

To further investigate the proposed model of origin of pancreatic cancer in the CAAC, we now present an extensive expression analysis and molecular characterization of the putative (i.e. TC, MTC) and established (i.e. PanIN) PDAC precursors in the *Kras*^{G12D/+};*Ptf1a-Cre*^{ex1/+} model and in a large collection human tissues, including three cases with familial PDAC background, this being the human condition that most closely resembles the mouse setting, which is characterized by the embryonic activation of a mutated *kras* from its endogenous locus.

Materials and methods

Animal and Clinical Specimens

LSL-Kras^{G12D}-mice were bred with *Ptf1a-Cre*^{ex1}-mice on a C57BL/6N background [6,18,19]. Double transgenic F1 offspring *LSL-Kras*^{G12D/+};*Ptf1a-Cre*^{ex1/+} (KPC) and wildtype (wt) control mice were sacrificed at 4, 9, 12, 18-24, 36 and 52 weeks (at least 4 mice/group). Serial sections (32-100) were cut. Each 10th slide was stained with haematoxylin and eosin (H&E) for morphological assessment; the remaining sections were set aside for further analyses. Morphological changes were classified according to established histological grading criteria [20]. All animal experiments were performed in compliance with the German animal welfare law and have been approved by the institutional committee on animal experimentation.

Formalin-fixed paraffin-embedded samples from a previously described human tissue collection [15] were used to construct tissue microarrays (TMA) using a manual tissue arrayer (Beecher Instruments, Sun Prairie, WI, USA) (table 1).

Pancreatic tissues from three patients who underwent prophylactic total pancreatectomy due to a familial PDAC background were included in the study (table S1).

The human tissues were retrieved from the archives of the Institute of Pathology of the University of Heidelberg, Germany and of the Technische Universität München, Germany, in accordance with local ethical regulation. Informed consent was obtained from all patients included in the study.

Immunohistochemistry

Immunohistochemistry was performed using an automated system (DiscoveryXT, Roche, Mannheim, Germany) with modified protocols for murine and human tissues (table S2 and supporting information).

Microdissection and genetic analysis of murine and human tissues

Genomic DNA from microdissected murine lesions was analyzed for the presence of *kras*^{G12D} activating dominant mutations following Cre-mediated recombination. In addition, the presence of mutations in exons 5-8 of *p53* and of deletion or promoter methylation of *p16^{Ink4a}/p19^{Arf}* locus were investigated (supporting information).

Mutation analysis of exon 2 of the *Kras* gene was performed in 6 sporadic PDAC samples and in 2 FPC samples after manual or laser microdissection of selected precursor lesions (supporting information).

Results

Histology

A detailed histological analysis of the human TMA tissues included in this study has been published elsewhere [15]. Briefly, pancreatic tissues displayed different degrees of acinar atrophy, accompanied by areas of ADM, with progressive flattening of acinar cells, lumen formation and appearance of small ductular structures (TC). In areas of ADM, TC displayed a progressive accumulation of supranuclear mucin and

enlargement of the lumen (MTC), thus becoming indistinguishable from low-grade PanIN lesions. High-grade PanIN were not observed in areas of ADM. Instead low- and high-grade PanIN were present in larger interlobular ducts not associated with ADM (figure 1A-C). A similar spectrum of lesions was observed in the pancreas of KPC mice. Multiple areas (up to 15% of the pancreas) of ADM with TC-MML-PanIN1 as well as a few mPanIN1 arising in pre-existing ducts were already present in 4 to 9 weeks-old mice. These changes progressively extended to almost replace the whole pancreas (77% of the tissue) by 36 weeks of age and were accompanied by increasing fibrosis and inflammation. A few mPanIN2 and mPanIN3 lesions were observed starting from 36 and 52 weeks, respectively (figure 1D-F). Three mice developed PDAC at the age of 18-52 weeks. Starting from 9 weeks, another type of flat lesion was observed in the murine tissues. These changes, which we define atypical flat lesions (AFL), were observed in areas of ADM and consisted of tubular structures lined by cuboidal cells with cytological atypia, namely enlarged nuclei with prominent nucleoli, high nuclear-cytoplasmic ratio and presence of mitoses (figure 2A-B). Interestingly, the presence of AFL in a tissue section could be easily identified at low magnification (i.e. without taking into account the cytological atypia) because of a peculiar appearance of the stroma surrounding the lesions. As shown in figure 2C-D, the stroma was loose but highly cellular with whorls of spindle cells that surrounded the tubular structures. The kinetic of the appearance of the different lesions with progressive age is shown in figure 2E.

The careful histological analysis of the pancreatic tissue of FPC patients revealed multiple PanIN and IPMN, mostly with low-grade but focally also with high-grade dysplasia. No invasive cancer was found. PanIN lesions were isolated (i.e. surrounded by otherwise normal parenchyma) or in areas of ADM, and areas of ADM

were not always associated with PanIN, thus suggesting that ADM can occur as a primary process independently of PanIN and is not necessarily related to a duct obstruction. In addition, flat ductular lesions with striking similarity to murine (m)AFL were seen in areas of ADM (figure 2F-I). Also in this case, human (h)AFL could be identified at low magnification by the peculiar aspect of the surrounding stroma (figure 2I).

Immunohistochemistry

Although originating in ADM areas, both murine and human AFL displayed a ductal phenotype, with only a few trypsin-positive cells retained in the human lesions (figure 3A-C). Muc1 was at least focally expressed in mAFL and mPDAC (figure 3D, figure 5C), hAFL were additionally positive for Muc5AC and negative for Muc2 (not shown). A transitional acinar to ductal phenotype was observed in ADM areas in TC and MTC/MML (figure 3A-F). Human centroacinar cells and TC also expressed Muc2 and 5AC (not shown). Human PanIN1-3 displayed a few trypsin-positive cells, as previously reported [15] (figure 4E-H).

The proliferative capacity of AFL was confirmed by the Ki-67 staining (figure 3G-H). In the mouse tissues, AFL were the only lesions to be predominantly (80%) proliferative active, with 22% of them showing a Ki-67 rate between 10 and 80% (table S3). All other lesions, including mPanIN, showed predominantly low (<10%) proliferation rates (figure 4M-N). This finding was confirmed in hAFL, which had similar proliferation rates of PanIN2 lesions of the same patient (figure 3H and 4R). The majority of TC and MTC had a proliferative index comprised between 1-5% (figure 3I). Twenty-five percent of mAFL and 36% of hAFL had more than 10% positive cells in the p53 immunostaining (figure 3J-K and table S3), whereas mPanIN

(figure 4O-P) and PanIN of FPC patients were mostly negative (figure 4U-V). The *Smad4* protein product was retained in all lesions except human sporadic PanIN3 (figure 3M-O, figure 4 a-b and g-j) and PDAC (table S3).

Since developmental pathways are often re-activated/dysregulated in carcinogenesis, the expression of Pdx1 and β -catenin was examined next. Pdx1 was extensively expressed in the mouse pancreas, but a reduction or loss of nuclear expression was observed in 60% of the AFL (figure 3P) and in PDAC (figure 5D). In human tissues only islets showed nuclear Pdx1 expression, whereas all other lesions, including AFL displayed cytoplasmic positivity (figure 3Q-R). Membranous β -catenin expression was retained in all lesions of human and mouse origin (not shown), thus confirming the notion of a functional Wnt signalling in the ductal carcinogenesis of the pancreas [21].

CK5 represents a basal and precursor cell marker in the human breast, which can give rise to both CK8/18-positive glandular elements and to smooth muscle actin-positive (SMA) myoepithelial cells [22]. Immunostaining for CK5 was therefore used to identify a possible subgroup of precursor cells and to follow their expression in the various precursor lesions. In the murine tissues a diffuse positivity of most lesions, including AFL, was observed (figure 3S). Interestingly, in human tissues, AFL, centroacinar cells and TC/MTC were strongly and diffusely positive for CK5 (figure 3T-U), whereas a basal cell staining was identified in low-grade PanIN (figure 4o, q). PanIN3 lesions (100%) (figure 4p, 3) and PDAC (86%, not shown) were diffusely positive for CK5.

Finally, the expression of α SMA was used as indicator of an activated stroma around lesions with possible precursor potential [23]. In the mouse tissue a stromal accumulation of α SMA was observed in 90% of the AFL and in the invasive cancers (figure 3V and 5F), whereas PanIN were negative (figure 4m, n). In the mouse tissues an extensive analysis of the inflammatory infiltrate using specific markers for macrophages, mast cells and B- and T-lymphocytes was additionally performed. Although all cell types accumulated in the lesional pancreas, only macrophages displayed a selective accumulation in the stroma of AFL and invasive cancers (not shown). In the human tissues, the perilesional stroma was generally positive for α SMA (figure 3W-X and figure 4s-v). The results of the immunohistochemical analysis are summarized in tables 2, 3 and S3.

Genetic analysis

In the mouse tissues PCR analysis confirmed the presence of *Cre*-recombined *kras*^{G12D} only in the pancreas, including microdissected AFL (figure S2). A strong promoter methylation or a deletion of exon 2 was found at the *p16^{Ink4a}/p19^{Arf}* locus, whereas no mutations of *p53* were observed (table 4 and figure 6).

Six cases of sporadic PDAC and the respective (putative) precursor lesions were investigated for the presence of *Kras* codon 12 and 13 mutations (table 5). Five out of 6 PDAC (83%) showed a codon 12 GGT→GAT transition, whereas in the remaining case a GGT→GTT transversion was found. All other lesions except one MTC and one PanIN2 displayed one or more mutations. Interestingly, in three cases the same mutation found in early putative precursors (TC/MTC) was present in the invasive cancer.

A *Kras* mutation analysis was additionally performed in some selected lesions of the FPC cases. Interestingly, *Kras* mutations were found both in human TC/MTC/AFL lesions and in classical precursor lesions (i.e. PanIN, IPMN) (figure S3).

Discussion

PanIN are well characterized precursors of PDAC. However, due to the difficulty to visualize them with imaging methods and consequently to gain biological material from patients with precursor lesions to be used for the purposes of early diagnosis, the clinical value of the accumulated knowledge about PanIN is still limited. The development of the first genetically defined mouse model of PDAC that fully recapitulates the complete morphological spectrum of the human disease has been therefore welcomed with great enthusiasm by the scientific community, providing the possibility to perform studies on early precursors of PDAC that are impossible on human tissues [6]. The number of low-grade mPanIN in the *LSL-Kras^{G12D/+};p48^{Cre}* mouse model exceeds that of high-grade lesions in all studies that tried a quantification of the tissue changes [24,25]. An accelerated progression to invasive cancer with metastatic disease is achieved when additional genetic changes are present, but an increase in the number of high-grade mPanIN is not reported in these settings [26,27]. Our analyses also show that mPanIN do not exhibit features that are found in mPDAC, such as increased proliferation, p53 dysregulation, loss of Pdx1 expression or stromal activation (tables 2 and 3). Instead, some of these features, together with exon 2 deletion or strong promoter methylation at the *p16^{Ink4a}/p19^{Arf}* locus, which belong to the earliest genetic changes of mPDAC [28], are found in mAFL. mAFL are ductal lesions that arise in ADM regions of the KPC mice from the age of 8 weeks and whose frequency increases with progressing age. To the best of our knowledge, AFL have not been described in this mouse model so far, but the

results of this study provide evidence that they actually could represent the most frequent site of origin of invasive cancer. Given the fact that AFL arise in regions of ADM, it could be speculated that they are part of a metaplasia-dysplasia-cancer sequence of the pancreas (figure 7), whose existence has already been suggested by others [29]. An interesting finding in this respect is the reduced expression of Pdx1 in mAFL and mPDAC, since Pdx1 has been previously implicated in metaplastic changes of the stomach and probably acts as a tumor-suppressor in gastric cancer [30,31].

Two important aspects have to be discussed at this point. First, one could argue that mAFL are just “small” PDAC, consisting of very few (sometimes only one) neoplastic gland (figure 2A, B). Disruption of the basal membrane and invasion of the surrounding tissue are hallmarks of invasive cancer, but they are very difficult to demonstrate at this very early stage. An aspect that argues against mAFL being small cancers is that they retain a lobular arrangement, whereas PDAC, even if small, is characterized by a haphazard distribution of the neoplastic glands (figure 5A). Secondly, the concept of AFL as precursors of PDAC in this mouse model does not intend to deny the PanIN-PDAC sequence, whose validity has been certainly proven for humans [3,4,8,32]. Instead, we suggest that AFL represent an additional form of precursor lesion, which can integrate the classical PanIN-PDAC pathway in the KPC mouse model.

The next fundamental issue is if a metaplasia-dysplasia-cancer sequence also takes place in the human pancreas and if lesions similar to mAFL can be identified in human tissues. This was actually the case in the pancreas of three patients with FPC background, in addition to PanIN and IPMN. Human AFL were associated with ADM,

as evidenced by the retained expression of trypsin in some of the cells, and of lobular atrophy, fibrosis and inflammation. These changes represent the so-called lobulocentric atrophy, which was described by Brune in the pancreas of patients with familial predisposition to PDAC [8], and has been included under the heading "precursor lesions" in the last classification of pancreatic tumours of the WHO [33]. The AFL's increased proliferation rate and nuclear expression of p53 when compared with low-grade PanIN of the same patient suggest a beginning dysregulation of the cell cycle in these lesions, which also harbour *Kras* mutations. Human AFL with the above described characteristics were not found in sporadic PDAC tissues, which were rich in ADM areas with TC and MTC. This could be due to a different molecular pathway of carcinogenesis in the two settings of sporadic and familial PDAC.

Nevertheless, TC and MTC in human sporadic and familial PDAC emerge from the present study as lesions with increasing proliferation and possible precursor potential, as evidenced by the strong expression of CK5 and by the co-expression of Muc1 and Muc2 (in TC), as well as by the presence of *Kras* mutations, which in half of the examined sporadic cases involved the same base pairs as in the associated invasive cancer. Additionally, only minor immunophenotypical differences between PanIN-like lesions in areas of ADM (MTC) and low-grade isolated PanIN (i.e. arising in pre-existing ducts) could be observed (table 3). Taken together, these results indicate regions of ADM in the mouse and human CAAC as the most probable site of origin of PDAC.

In conclusion, the present extensive analysis of the pancreas of KPC mice and of patients with sporadic PDAC and FPC background shows that ADM is a frequent finding and represents a region of increased proliferation, de- and redifferentiation

and metaplasia, whose role in the carcinogenesis of the pancreas still remains to be defined. ADM-associated AFL are the most probable precursors of PDAC in the *Kras*^{G12D/+};*Ptf1a-Cre*^{ex1/+} mice in alternative to PanIN, whose contribution to carcinogenesis has to be reconsidered in this genetically engineered mouse model. Further studies are warranted to clarify the malignant potential of AFL in humans and their relation to the classical PanIN-PDAC pathway.

Acknowledgments

This work was partly supported by grants from the Wilhelm Sander-Stiftung (No. 2008.021.1) to I.E. and K.M.D., and from the Deutsche Forschungsgemeinschaft (SFB824 TP Z2) to I.E.

The authors would like to thank Prof. R. Schmid (Dep. of Internal Medicine II, Technische Universität München, Germany) for providing the *LSL-Kras*^{G12D} and the *Ptf1a-Cre*^{ex1} mouse strains.

We are grateful to Prof. Jörg Kleeff and Dr. Christoph Michalski (Department of Surgery, Technische Universität München, Munich, Germany) for valuable suggestions on the manuscript and to Vesna Vukovic, Jacqueline Müller, Waldemar Schneider, Daniela Angermeier and Birgit Geist for excellent technical assistance.

Dr. Igor Paron is acknowledged for his contribution to establish the PCR-based assay for the detection of *kras*^{G12D} activating dominant mutation in the mouse tissues.

The monoclonal antibody TROMA-III developed by Rolf Kemler (Max-Planck Institute, Freiburg, Germany) was obtained from the Developmental Study Hybridoma Bank developed under the auspices of the NICHD and maintained by The University of Iowa, Department of Biology, Iowa City, IA 52242.

Authors' contributions

MA, CS, MT, JS conceived and carried out experiments, PKM, PDS, SC, AD carried out experiments, DB, PL collected and analyzed data, JS, HH, GK, KMD conceived experiments and analyzed data, MB and IE designed the study, analyzed data and wrote the manuscript. All authors had final approval of the submitted version.

List of online supporting information

1. Material and Methods: Immunohistochemistry and Morphometric analysis, Genetic analysis of murine tissues, Microdissection and mutation analysis of human tissues
2. TableS1: Clinical data and selection criteria of three patients with FPC background
3. Table S2 Antibodies and protocols for immunohistochemistry
4. Table S3 Quantification of immunohistochemical parameters
5. Figure S1: Mouse genotyping scheme
6. Figure S2: Genetic analysis of mouse tissues
7. Figure S3: Genetic analysis of a microdissected lesion in a FPC patient

References

1. Jemal A, Siegel R, Xu J, *et al.* Cancer statistics, 2010. *CA Cancer J Clin* 2010; **60**: 277-300
2. Lim JE, Chien MW, Earle CC. Prognostic factors following curative resection for pancreatic adenocarcinoma: a population-based, linked database analysis of 396 patients. *Ann Surg* 2003; **237**: 74-85
3. Kloppel G, Bommer G, Ruckert K, *et al.* Intraductal proliferation in the pancreas and its relationship to human and experimental carcinogenesis. *Virchows Arch A Pathol Anat Histol* 1980; **387**: 221-233
4. Sipos B, Frank S, Gress T, *et al.* Pancreatic intraepithelial neoplasia revisited and updated. *Pancreatology* 2009; **9**: 45-54
5. Hruban RH, Adsay NV, Albores-Saavedra J, *et al.* Pancreatic intraepithelial neoplasia: a new nomenclature and classification system for pancreatic duct lesions. *Am J Surg Pathol* 2001; **25**: 579-586
6. Hingorani SR, Petricoin EF, Maitra A, *et al.* Preinvasive and invasive ductal pancreatic cancer and its early detection in the mouse. *Cancer Cell* 2003; **4**: 437-450
7. Lohr M, Kloppel G, Maisonneuve P, *et al.* Frequency of K-ras mutations in pancreatic intraductal neoplasias associated with pancreatic ductal adenocarcinoma and chronic pancreatitis: a meta-analysis. *Neoplasia* 2005; **7**: 17-23
8. Brune K, Abe T, Canto M, *et al.* Multifocal neoplastic precursor lesions associated with lobular atrophy of the pancreas in patients having a strong family history of pancreatic cancer. *Am J Surg Pathol* 2006; **30**: 1067-1076
9. Shi C, Klein AP, Goggins M, *et al.* Increased Prevalence of Precursor Lesions in Familial Pancreatic Cancer Patients. *Clin Cancer Res* 2009; **15**: 7737-7743
10. Maitra A, Hruban RH. Pancreatic cancer. *Annu Rev Pathol* 2008; **3**: 157-188

11. Guerra C, Schuhmacher AJ, Canamero M, *et al.* Chronic pancreatitis is essential for induction of pancreatic ductal adenocarcinoma by K-Ras oncogenes in adult mice. *Cancer Cell* 2007; **11**: 291-302
12. Habbe N, Shi G, Meguid RA, *et al.* Spontaneous induction of murine pancreatic intraepithelial neoplasia (mPanIN) by acinar cell targeting of oncogenic Kras in adult mice. *Proc Natl Acad Sci U S A* 2008; **105**: 18913-18918
13. Stanger BZ, Stiles B, Lauwers GY, *et al.* Pten constrains centroacinar cell expansion and malignant transformation in the pancreas. *Cancer Cell* 2005; **8**: 185-195
14. Strobel O, Dor Y, Alsina J, *et al.* In vivo lineage tracing defines the role of acinar-to-ductal transdifferentiation in inflammatory ductal metaplasia. *Gastroenterology* 2007; **133**: 1999-2009
15. Esposito I, Seiler C, Bergmann F, *et al.* Hypothetical progression model of pancreatic cancer with origin in the centroacinar-acinar compartment. *Pancreas* 2007; **35**: 212-217
16. Zhu L, Shi G, Schmidt CM, *et al.* Acinar cells contribute to the molecular heterogeneity of pancreatic intraepithelial neoplasia. *Am J Pathol* 2007; **171**:263-273
17. Wellings SR, Jensen HM, Marcum RG. An atlas of subgross pathology of the human breast with special reference to possible precancerous lesions. *J Natl Cancer Inst* 1975; **55**: 231-273
18. Nakhai H, Sel S, Favor J, *et al.* Ptf1a is essential for the differentiation of GABAergic and glycinergic amacrine cells and horizontal cells in the mouse retina. *Development* 2007; **134**: 1151-1160
19. Algul H, Treiber M, Lesina M, *et al.* Pancreas-specific RelA/p65 truncation increases susceptibility of acini to inflammation-associated cell death following cerulein pancreatitis. *J Clin Invest* 2007; **117**: 1490-1501

20. Hruban RH, Adsay NV, Albores-Saavedra J, *et al.* Pathology of genetically engineered mouse models of pancreatic exocrine cancer: consensus report and recommendations. *Cancer Res* 2006; **66**: 95-106
21. Morris JPt, Cano DA, Sekine S, *et al.* Beta-catenin blocks Kras-dependent reprogramming of acini into pancreatic cancer precursor lesions in mice. *J Clin Invest* 2010; **120**: 508-520
22. BoeckerW, Buerger H. Evidence of progenitor cells of glandular and myoepithelial cell lineages in the human adult female breast epithelium: a new progenitor (adult stem) cell concept. *Cell Prolif* 2003; **36** Suppl 1:73-84
23. Erkan M, Michalski CW, Rieder S, *et al.* The activated stroma index is a novel and independent prognostic marker in pancreatic ductal adenocarcinoma. *Clin Gastroenterol Hepatol* 2008; **6**: 1155-1161
24. Khasawneh J, Schulz MD, Walch A, *et al.* Inflammation and mitochondrial fatty acid beta-oxidation link obesity to early tumor promotion. *Proc Natl Acad Sci U S A* 2009; **106**: 3354-3359
25. Gidekel Friedlander SY, Chu GC, Snyder EL, *et al.* Context-dependent transformation of adult pancreatic cells by oncogenic K-Ras. *Cancer Cell* 2009; **16**: 379-389
26. Hingorani SR, Wang L, Multani AS, *et al.* Trp53R172H and KrasG12D cooperate to promote chromosomal instability and widely metastatic pancreatic ductal adenocarcinoma in mice. *Cancer Cell* 2005; **7**: 469-483
27. Bardeesy N, Aguirre AJ, Chu GC, *et al.* Both p16(Ink4a) and the p19(Arf)-p53 pathway constrain progression of pancreatic adenocarcinoma in the mouse. *Proc Natl Acad Sci U S A* 2006; **103**: 5947-5952

28. Mazur PK, Einwächter H, Lee M, *et al.* Notch2 is required for progression of pancreatic intraepithelial neoplasia and development of pancreatic ductal adenocarcinoma. *Proc Natl Acad Sci U S A* 2010; **107**:13438-43.
29. Murtaugh LC, Leach SD. A case of mistaken identity? Noductal origins of pancreatic "ductal" cancers. *Cancer Cell* 2007; **11**: 211-213
30. Sakai H, Eishi Y, Li XL, *et al.* PDX1 homeobox protein expression in pseudopyloric glands and gastric carcinomas. *Gut* 2004; **53**: 323-330
31. Ma J, Wang JD, Zhang WJ, *et al.* Promoter hypermethylation and histone hypoacetylation contribute to pancreatic-duodenal homeobox 1 silencing in gastric cancer. *Carcinogenesis* 2010; **31**: 1552-1560
32. Liszka L, Pajak J, Mrowiec S, *et al.* Precursor lesions of early onset pancreatic cancer. *Virchows Arch* 2011; **458**: 439-451
33. Bosman FT, Carneiro F, Hruban RH, *et al.* (Eds.). WHO Classification of Tumours of the Digestive System. IARC:Lyon 2010

Table 1. Composition of the tissue microarrays

| | Lesion included | | N° of cores | N° of cases |
|--------------|------------------------|-------------------------------------|------------------------|------------------------|
| TMA 1 | TC/MTC | | 52 | 24 |
| TMA 2 | TC/MTC | | 44 | 20 |
| TMA 3 | PanIN | 22 PanIN1 13 PanIN2 14 PanIN3 | 49 | 39 |
| TMA 4 | PDAC | | 171 | 57 |

Table 2. Comparative immunohistochemical profile of human and mouse AFL and mouse PDAC.

| | Human AFL | Mouse AFL | Mouse PDAC |
|------------------------|-----------|-----------|------------|
| Trypsin/Amylase | - | - | - |
| Muc1 | + | + | + |
| Mib1 | + | + | + |
| p53 | + | - | + |
| Smad4 | + | + | + |
| Pdx1 | + (c) | -/+ | -/+ |
| CK5 | + | + | + |
| αSMA | + | + | + |

+ and – refers to the predominant (i.e. positive of negative) expression pattern without quantification.

-/+ describes the loss of expression observed in mouse AFL and PDAC compared to the relatively strong positivity observed in all other murine lesions (see text for details). c= cytoplasmic staining.

Table 3. Immunohistochemical analysis of the precursor lesions in human and murine specimens

| Marker | Specimen | TC | MTC ⁺ / | PanIN | PanIN |
|------------------------|--------------------|----|--------------------|-----------|------------|
| | | | MML | low-grade | high-grade |
| Trypsin/Amylase | Human sporadic | + | - | +/- | - |
| | Human familial | + | - | +/- | - |
| | Mouse | + | - | - | - |
| Muc1 | Human sporadic | + | - | + | + |
| | Human familial | + | +/- | + | + |
| | Mouse | + | + | + | + |
| Mib1 | Human sporadic (c) | + | + | + | + |
| | Human familial (c) | + | + | + | + |
| | Mouse (n) | - | - | - | - |
| p53 | Human sporadic | - | - | - | + |
| | Human familial | - | - | - | - |
| | Mouse | - | - | - | - |
| Smad4 | Human sporadic | + | + | + | - |
| | Human familial | + | + | + | + |
| | Mouse | + | + | + | + |
| Pdx1 | Human sporadic | + | + | + | + |
| | Human familial | + | + | + | + |
| | Mouse | + | + | + | + |
| CK5 | Human sporadic | + | + | + | + |
| | Human familial | + | + | + | + |
| | Mouse | + | + | + | + |
| αSMA | Human sporadic | + | + | + | ++ |
| | Human familial | + | + | + | + |
| | Mouse | + | - | - | - |

For trypsin/amylase, Muc1, Pdx1, CK5: + expression in >10% of the cells in more than 50% of the analyzed lesions; +/- expression in >10% of the cells in 50% of the lesions; - expression in \leq 10% of the cells in more than 50% of the lesions. c: cytoplasmic staining; n: nuclear staining.

For Mib1, p53 and Smad4: + and – refers to the predominant (i.e. positive or negative) expression pattern without quantification. For quantification see table S3.

For α SMA: + weak to moderate stromal expression; ++ strong stromal expression; - no expression

*MTC are morphologically indistinguishable from low-grade PanIN occurring in pre-existing ducts

Table 4. Molecular analysis of microdissected murine lesions.

| Sample | <i>p16^{Ink4}</i> methylation | <i>p16^{Ink4a}</i> gene inactivation | <i>p19^{Arf}</i> gene inactivation | <i>p53</i> gene mutation |
|--------|--|---|---|-----------------------------|
| M222 | + | N | N | N |
| W36 | + | N | N | N |
| M172 | +/- | Y | Y | N |
| W270 | +/- | Y | Y | N |

Y, yes; N, no; +/-, weak promoter methylation detected; +, robust promoter methylation detected

Table 5. *K-ras* mutation analysis in sporadic PDAC cases and precursor lesions

| Case | TC/ small MTC | Large MTC | PanIN1 | PanIN2 | PanIN3 | PDAC |
|-------------|--------------------------|------------------|---------------|---------------|---------------|-------------|
| 1 | CGT | CGT | GAT | wildtype | GAT | GAT |
| 2 | GAT | GAT | GAT | - | - | GAT |
| 3 | CGT/GTT | wildtype | - | - | - | GTT |
| 4 | GAT/GTT | GAT | CGT | - | - | GAT |
| 5 | GTT | GTT | GAT/GTT | GAT | GAT | GAT |
| 6 | CGT/GTT | CGT | GAT | GTT | GAT | GAT |

Figure legends

Figure 1

Representative pictures of areas of acinar-ductal metaplasia (ADM; A and D), low-grade (B and E) and high-grade PanIN (C and F) encountered in human (A-C) and murine (D-F) tissues. Inset A shows a detail of mucinous tubular complexes (MTC) in human ADM.

Figure 2

Atypical flat lesions in murine (A-D) and human pancreas (F-I) of FPC-patients. AFL present as tubular structures with enlarged and hyperchromatic nuclei in areas of ADM. The dotted areas in A and F are shown at higher magnification in B and G, respectively, highlighting the atypical cytological features of the lesion. The tubular structures are surrounded by a fibrous and cellular stroma, which sometimes has a myxoid appearance (C and I). The high content in glycosaminoglycans is highlighted in the Alcian blue-PAS staining (D). E shows the frequency of AFL and high-grade PanIN lesions (PanIN3), expressed as number of lesions/mouse (y-axis) in the different age groups (x-axis: weeks). The shadowed area represents the time frame in which pancreatic cancer was detected in this cohort of mice.

Figure 3

Immunohistochemical characterization of atypical flat lesions and of acinar-ductal metaplasia in the *LSL-Kras^{G12D/+};Ptf1a-Cre^{ex1/+}* mice (left column) and in patients with familial pancreatic cancer background (middle column) and sporadic pancreatic cancer (right column).

A: Double staining for **CK19** (red) and **amylase** (brown) highlights the ductal and acinar components in mADM. AFL (arrows) display only ductal differentiation. **B, C:** In the human tissues, **trypsin** is clearly identified in the acinar component of ADM areas and in TC/MTC. **D-F:** **Muc1** is expressed at least focally in murine and human TC/AFL. MTC (F, arrow) are negative. **G-I:** **Ki-67** reveals the proliferative character of murine and human AFL (G, H) and of hTC (I). **J-L:** **p53** is focally expressed in murine and human AFL (J, K) and in hTC (L). **M-O:** **Smad4** is expressed in murine (M) and human AFL (N), as well as in TC (O). **P-R:** Reduced nuclear expression of **Pdx1** in mAFL (P). Multifocal to diffuse cytoplasmic staining is found in all analysed human lesions (Q, R), without differences between familial and sporadic cases. Arrows in Q and R indicate positive nuclear staining of islet cells. **S-U:** **CK5** shows a diffuse cytoplasmic staining in murine and human TC/AFL. **V-X:** **αSMA** is expressed in the stroma surrounding mAFL (V) and hTC/AFL (W, X).

Figure 4

Immunohistochemical characterization of murine and human PanIN lesions. For the human lesions, FPC cases are presented in the two left columns and sporadic cases in the two right columns.

A, B: Double immunostaining for amylase (brown) und CK19 (red) in low-grade mPanIN (A) showing an exclusively ductal differentiation. High-grade mPanIN (B) diffusely express CK19 (brown) too. **C, D:** Muc1-expression in mPanIN. **E-L:** Low- (E, G, I, K) and high-grade (F, H, J, L) PanIN in patients with familial and sporadic pancreatic cancer displaying partial trypsin positivity (E-H) and focal to diffuse Muc1 expression (I-L). **M-P:** Focal Ki-67 staining (M-N) and absence of p53 expression (O-P) in low- and high-grade mPanIN. **Q-X:** Ki-67-proliferating activity (Q-T) and p53 expression (U-X) in hPanIN. High-grade PanIN show a moderate to strong

proliferation (R, T). p53 overexpression is only seen in some sporadic high-grade PanIN (X). **Y-b** Diffuse nuclear expression of Pdx1 (Y-Z) and retained expression Smad4 in mPanIN (a-b). **c-f**: Cytoplasmic expression of Pdx1 in low- and high-grade hPanIN. **g-j**: Human low- and high-grade PanIN mostly show retained expression of Smad4 (g-i). Only some sporadic high-grade lesions (j) display loss of expression. **k-n**: Cytoplasmic staining for CK5 (k-l) and absence of α SMA staining in mPanIN (m-n). Blood vessels served as internal positive control for the α SMA staining. **o-r**: CK5 staining in hPanIN showing a basal cell pattern in low-grade (o, q) and a more diffuse cytoplasmic staining in high-grade lesions (p, r). **s-v**: α SMA staining shows a positive stroma around low- and high-grade hPanIN.

Figure 5

Histology and immunohistochemical characterization of small murine PDAC.

A: Overview of a small PDAC detected through serial sectioning of the entire pancreatic gland. **B**: Detail of PDAC showing atypical glands embedded in a desmoplastic stroma, thus closely resembling human PDAC. **C**: **Muc1** staining of the neoplastic glands. **D**: **Pdx1** nuclear staining of incipient PDAC (arrows) depicting the reduction/loss of expression compared to the strong positivity of surrounding parenchyma. **E**: Active proliferation of the neoplastic glands in the **Ki-67** staining. **F**: Retained **Smad4** expression in the tumour tissue **G**: Peritumoral stromal reaction evidenced by **α SMA** staining.

Figure 6

A. Methylation-specific PCR analysis of $p16^{Ink4a}$ promoter. DNA specimens were treated with bisulfite and analyzed by PCR using primers that recognize methylated (M) or unmethylated (U) sequences in the $p16^{Ink4a}$ 5'UTR regulatory region. The

specificity of the primers was confirmed by the lack of amplification of DNA that was not subjected to bisulfite treatment (unmodified). **B.** Results of $p16^{Ink4a}/p19^{Arf}$ locus deletion analysis. Amplification of $p16^{Ink4a}$ Exon1a (ex1a), common $p16^{Ink4a}$ and $p19^{Arf}$ exon 2 (ex2) and $p19^{Arf}$ exon 1b (ex1b) indicate locus status in the analyzed samples.

Figure 7

Proposed model of pancreatic carcinogenesis based on the results of the present study (A, mouse; B, human).

The origin of PDAC is set in the centroacinar-acinar compartment, where tubular complexes originate. Loss of acinar differentiation with acquisition of a CK19+/Muc1+ ductal phenotype, increased proliferation (star) and atypia with p16/p19 dysregulation (black circle), and an increasing stromal reaction characterize the alternative “flat” progression model, where AFL represent direct PDAC precursors. The classical “mucinous” pathway includes mucinous metaplastic lesions/mucinous tubular complexes as PanIN and PDAC precursors. Empty symbols indicate weak/reduced expression, missing symbols indicate loss of expression.

Supporting information

Material and Methods

Immunohistochemistry and Morphometric analysis

The tissue sections were deparaffinized, rehydrated, and subjected to peroxidase block and antigen retrieval, if required. To block nonspecific antibody binding, blocking serum (KPL, Kirkegaard and Perry Laboratories, Gaithersburg, MD, USA) was applied for 30 minutes. Isotype-matched IgG served as negative controls. The list of the antibodies used in this study and the respective protocols are provided in table S2.

Slides were scanned at 20x magnification using the dotSlide digital virtual microscopy system (Olympus, Hamburg, Germany). The total area as well as the surface of an individual region of interest was measured. Moreover, quantification of specific markers (Ki67, p53, Smad4) was performed. In detail, AFL, mouse and human PanIN were identified on the slide. The percentage of positive cells in each lesion was determined. For α -SMA and Mac3 a semi-quantitative approach was chosen and the lesions were classified into negative (-), positive (+) and strong positive (++) according to the staining intensity.

Recombination analysis of murine tissues

Genomic DNA was extracted from mouse tails and from paraffin-embedded tissues (whole liver, whole pancreas and microdissected precursor lesions), then PCR was performed under standard conditions using following sets of primers:

K004: 5'-GTCGACAAGCTCATGCGGGTG-3';

KrasSD5: 5'-AGCTAGCCACCATGGCTTGAGTAAGTCTGCA-3';

KrasFw1:5'-GTCTTTCCCCAGCACAGTGCA-3';

K006 : 5'-CCTTTACAAGCGCACGCAGACTGTAGA-3'

in order to identify: 1) Kras wild-type allele; 2) Kras^{G12D} allele, not recombined; 2) Kras^{G12D} allele, recombined (figure S1).

Genetic analysis of murine AFL

p53 mutation analysis

Genomic DNA from microdissected lesions were analyzed for presence of mutations in *p53* exons 5-8 corresponding to DNA-binding domain of p53 protein. Briefly, sequences were amplified using Platinum High Fidelity Polymerase (Invitrogen) in touchdown PCR conditions: 5 min at 95°C; 20 cycles of denaturation at 94°C for 30 s, annealing at 65°C -0.5°C/cycle for 30 s, extension at 72°C for 1 min; followed by 25 cycles of denaturation at 94°C for 30 s, annealing at 45°C for 30 s, extension at 72°C for 1 min and 10 min final extension at 72°C. Following primers were utilized: Exon 5 (214 bp product): mp53-ex5-F TCTCTTCCAGTACTCTCCTC; mp53-ex5-R AGGCGGTGTTGAGGGCTTAC; Exon 6 (181 bp product): mp53-ex6-F GGCTTCTGACTTATTCTTGC; mp53-ex6-R CAACTGTCTCTAAGACGCAC; Exon 7 (170 bp product): mp53-ex7-F TCACCTGGATCCTGTGTCTT; mp53-ex7-R CAGGCTAACCTAACCTACCA; Exon 8 (279 bp product): mp53-ex8-F ACTGCCTTGTGCTGGTCCTT; mp53-ex8-R GGAGAGGCGCTTGTGCAGGT. PCR reactions were run on 2% agarose gels. Each PCR product was isolated using QIAquick Gel Extraction Kit (Qiagen) and sequenced using respective 3' primer.

p16^{Ink4a}/p19^{Arf} locus deletion status

Genomic DNA isolated from microdissected lesions and p16^{Ink4a}/p19^{Arf} locus was amplified in a touchdown PCR using JumpStart polymerase (Sigma) under following conditions: 5 min at 95°C; 20 cycles of denaturation at 94°C for 30 s, annealing at 63°C -0.5°C/cycle for 30 s, extension at 72°C for 1 min; followed by 25 cycles of

denaturation at 94°C for 30 s, annealing at 50°C for 30 s, extension at 72°C for 1 min and 10 min final extension at 72°C. Following primers were used for mouse $p16^{Ink4a}$ exon 1a: p16-ex1a-F ATGGAGTCCGCTGCAGACAG; p16-ex1a-R CTGAATCGGGGTACGACCGA (126bp product) and exon 2: p16-ex2-F GTGATGATGATGGGCAACGT; p16-ex2-R TGGGCGTGCTTGAGCTGAAG (340bp product) and for $p19^{ARF}$ exon 1b: p19-ex1b-F TACAGCAGCGGGAGCATGGGT; p19-ex1b-R CTGGTCCAGGATTCCGGT (205bp product). PCR reactions were run on 2% agarose gels. Lack of expected products was interpreted as a locus deletion.

Methylation-specific PCR analysis of $p16^{Ink4a}$ promoter

Promoter methylation status of $p16^{Ink4a}/p19^{ARF}$ locus was analyzed as described before [28]. Briefly, genomic DNA isolated from microdissected lesions was treated with bisulfite using the EpiTect Bisulfite kit (Qiagen). The modified DNA was eluted with a final volume of 16 μ l, and 2 μ l were used for the methylation specific polymerase chain reactions (MSP) utilizing JumpStart polymerase (Sigma). The PCR was performed in a 20 μ l reaction subjected to hot start at 85°C and the touchdown conditions: 5 min at 95°C; 20 cycles of denaturation at 94°C for 30 s, annealing at 65°C -0.5°C/cycle for 30 s, extension at 72°C for 1 min; followed by 25 cycles of denaturation at 94°C for 30 s, annealing at 50°C for 30 s, extension at 72°C for 1 min and 10 min final extension at 72°C. PCR products were separated by electrophoresis 2% agarose gel and visualized by staining with ethidium bromide. Methylated alleles of the $p16^{Ink4a}$ promoter were amplified with following primers: p16-Methylated-F CGATTGGGCGGGTATTGAATTTTCGC; p16-Methylated-R CACGTCATACACACGACCCTAAACCG. Unmethylated alleles were amplified with primers: p16-Unmethylated-F GTGATTGGGTGGGTATTGAATTTTGTG; p16-

Unmethylated-R CACACATCATAACACACAACCCTAAACCA. Primers to unmodified DNA were used as a control for complete bisulfite modification of the treated DNA.

Microdissection and mutation analysis of human tissues

Six cases of sporadic PDAC that included a wide spectrum of putative precursor lesions, as well as two cases with familial pancreatic cancer background were selected for further genetic analysis. Manual or laser microdissection with the PALM[®] Microbeam Laser Microdissector (P.A.L.M. Microlaser Technologies, Bernried, Germany) was performed on sections from formalin-fixed, paraffin-embedded tissues. Genomic DNA was isolated using the QIAamp DNA Mini Kit (Qiagen, Germany). Exon 2 of the *Kras* gene that contains the codons 12 and 13 was amplified by PCR under standard conditions and the purified PCR products were sequenced directly in the forward and reverse directions on an ABIPrism 377-18 DNA sequencer (Applied Biosystems, Foster City, CA, USA) using the BigDye Termination Kit (Applied Biosystems).

Table S1.**Clinical data and selection criteria of three patients with FPC background**

| Patient ID | Gender | Age | History of PDAC | BRCA2 | PALB2 | Other |
|-------------------|---------------|------------|---|--------------|--------------|--|
| 1 | F | 65 | 1 FDR (father), 1 other relative | wt | wt | Breast cancer, suggestive findings in MRCP |
| 2 | F | 52 | 2 FDR (mother and sister) 2 other relatives | wt | wt | 3 cases of breast cancer in the family |
| 3 | F | 58 | 2 FDR (twin-sister and brother) | wt | wt | |

FDR: first-degree relative; MRCP: magnetic resonance cholangiopancreatography

Table S2**Antibodies and protocols for immunohistochemistry**

| Antibody (clone) Company | Dilution | Antigen retrieval | Use |
|--|-----------------|--------------------------|-----------------|
| Trypsin Immune System Limited (Paignton, UK) | 1:100 | none | human |
| Amylase Sigma (Taufkirchen, Germany) | 1:1000 | citrate buffer, pH6 | mouse |
| CK19 developmental studies hybridoma bank, IOWA University | 1:250 | EDTA buffer, pH8 | mouse |
| CK5 (24647) Abcam (Cambridge, UK) | 1:100 | enzymatic | human and mouse |
| PDX-1 Abcam | 1:2000 | citrate buffer, pH6 | human and mouse |

| | | | |
|---|------------------|---|-------|
| Ki-67 (MIB1) Dako (Hamburg, Germany) | 1:200 | Antigen retrieval solution pH 6 (Dako) | human |
| Ki-67 (SP6) DCS (Hamburg, Germany) | Ready- to-use | citrate buffer, pH6 | mouse |

| | | | |
|---|--------|---|-----------------|
| p53 Novocastra/Menarini Diagnostics (Berlin, Germany) | 1:100 | Antigen retrieval solution pH 6 (Dako) | human and mouse |
| Smad4 (B8) SantaCruz Biotechnology (Santa Cruz, CA, USA) | 1:50 | citrate buffer, pH6 | human and mouse |
| Muc-1 (Ma695) Novocastra | 1:100 | citrate buffer, pH6 | human |
| Muc-1 (ab5) Labvision | 1:100 | EDTA buffer, pH8 | mouse |
| Muc-2 (CCP58) Novocastra | 1:100 | citrate buffer, pH6 | human |
| Muc-5AC (CLH2) Chemicon (Temecula, CA) | 1:1000 | | |

Table S3

Quantification of immunohistochemical parameters.

Ki-67

mouse

| <i>Type of lesion</i> | <i>n</i> | <i>negative</i> | <i><10%</i> | <i>10-80%</i> | <i>>80%</i> |
|-----------------------|----------|-----------------|----------------|---------------|----------------|
| AFL | 200 | 40 (20%) | 115 (58%) | 45 (22%) | 0 |
| mPanIN1 | 182 | 126 (69%) | 48 (26%) | 8 (4%) | 0 |

| | | | | | |
|----------------|---|----------|----------|----------|---|
| mPanIN2 | 4 | 4 (100%) | 0 | 0 | 0 |
| mPanIN3 | 1 | 0 | 1 (100%) | 0 | 0 |
| mPDAC | 3 | 0 | 0 | 3 (100%) | 0 |

human-FPC

| <i>Type of lesion</i> | <i>n</i> | <i>negative</i> | <i><10%</i> | <i>10-80%</i> | <i>>80%</i> |
|-----------------------|----------|-----------------|----------------|---------------|----------------|
| AFL | 20 | 5 (25%) | 7 (35%) | 7 (35%) | 1 (5%) |
| hPanIN1 | 17 | 0 | 17 (100%) | 0 | 0 |
| hPanIN2 | 3 | 0 | 1 (33%) | 2 (66%) | 0 |
| hPanIN3 | - | | | | |
| hPDAC | - | | | | |

human-sporadic

| <i>Type of lesion</i> | <i>n</i> | <i>negative</i> | <i><10%</i> | <i>10-80%</i> | <i>>80%</i> |
|-----------------------|----------|-----------------|----------------|---------------|----------------|
| AFL | - | | | | |
| hPanIN1 | 6 | 0 | 3 (50%) | 3 (50%) | 0 |
| hPanIN2 | 6 | 0 | 1 (17%) | 5 (83%) | 0 |
| hPanIN3 | 10 | 0 | 0 | 10 (100%) | 0 |
| hPDAC | n.d. | | | | |

n.d. not determined

p53

mouse

| <i>Type of lesion</i> | <i>n</i> | <i>negative</i> | <i><10%</i> | <i>10-80%</i> | <i>>80%</i> |
|-----------------------|----------|-----------------|----------------|---------------|----------------|
| AFL | 158 | 91 (58%) | 28 (18%) | 39 (25%) | 0 |
| mPanIN1 | 49 | 49 (100%) | 0 | 0 | 0 |
| mPanIN2 | 3 | 3 (100%) | 0 | 0 | 0 |
| mPanIN3 | 2 | 2 (100%) | 0 | 0 | 0 |
| mPDAC | 2 | 0 | 0 | 2 (100%) | 0 |

human-FPC

| <i>Type of lesion</i> | <i>n</i> | <i>negative</i> | <i><10%</i> | <i>10-80%</i> | <i>>80%</i> |
|-----------------------|----------|-----------------|----------------|---------------|----------------|
| AFL | 11 | 3 (27%) | 4 (36%) | 4 (36%) | 0 |
| hPanIN1 | 18 | 9 (50%) | 9 (50%) | 0 | 0 |
| hPanIN2 | 2 | 2 (100%) | 0 | 0 | 0 |
| hPanIN3 | - | | | | |
| hPDAC | - | | | | |

human-sporadic

| <i>Type of lesion</i> | <i>n</i> | <i>negative</i> | <i><10%</i> | <i>10-80%</i> | <i>>80%</i> |
|-----------------------|----------|-----------------|----------------|---------------|----------------|
| AFL | - | | | | |
| hPanIN1 | 7 | 7 (100%) | 0 | 0 | 0 |
| hPanIN2 | 6 | 2 (33%) | 0 | 1 (17%) | 3 (50%) |
| hPanIN3 | 8 | 4 (50%) | 0 | 2 (25%) | 2 (25%) |
| hPDAC | 52 | 18 (35%) | 0 | 11 (21%) | 23 (44%) |

Smad4

mouse

| <i>Type of lesion</i> | <i>n</i> | <i>negative</i> | <i><50%</i> | <i>50-80%</i> | <i>>80%</i> |
|-----------------------|----------|-----------------|----------------|---------------|----------------|
| AFL | 26 | 0 | 1 (4%) | 5 (19%) | 20 (77%) |
| mPanIN1 | 26 | 0 | 0 | 7 (27%) | 19 (73%) |
| mPanIN2 | 6 | 0 | 0 | 4 (67%) | 2 (33%) |
| mPanIN3 | 2 | 0 | 0 | 1 (50%) | 1 (50%) |
| mPDAC | 2 | 0 | 0 | 1 (50%) | 1 (50%) |

human-FPC

| <i>Type of lesion</i> | <i>n</i> | <i>negative</i> | <i><50%</i> | <i>50-80%</i> | <i>>80%</i> |
|-----------------------|----------|-----------------|----------------|---------------|----------------|
| AFL | 9 | 0 | 5 (56%) | 2 (22%) | 2 (22%) |
| hPanIN1 | 11 | 0 | 0 | 2 (18%) | 9 (82%) |
| hPanIN2 | 5 | 0 | 0 | 3 (60%) | 2 (40%) |
| hPanIN3 | - | | | | |
| hPDAC | - | | | | |

human-sporadic

| <i>Type of lesion</i> | <i>n</i> | <i>negative</i> | <i><50%</i> | <i>50-80%</i> | <i>>80%</i> |
|-----------------------|----------|-----------------|----------------|---------------|----------------|
| AFL | - | | | | |
| hPanIN1 | 6 | 0 | 5 (84%) | 1 (16%) | 0 |
| hPanIN2 | 4 | 0 | 3 (75%) | 1 (25%) | 0 |
| hPanIN3 | 6 | 4 (67%) | 0 | 0 | 2 (33%) |
| hPDAC | 43 | 38 (88%) | 1 (2.5%) | 1 (2.5%) | 3 (7%) |

Supporting information

Figure S2

PCR-detection of the wild-type, not recombined and recombined *kras*^{G12D} allele in the *LSL-Kras*^{G12D/+};*Ptf1a-Cre*^{ex1/+} mice. DNA was extracted from the whole liver and pancreas, as well as from microdissected PDAC and precursor lesions and from the

mouse tail. a) Primers K004/K006, product: 522 bp, all three alleles are detected. b) Primers *Kras*SD5/K006, product 601 bp, *Kras*^{G12D} not recombined. c) Primers *Kras*Fw1/K006, product 761 bp *Kras*^{G12D}*Cre* recombined (above), product 721 bp wild-type allele (below). Lane 1: negative control, lane 2: liver, lane 3: whole pancreas, lane 4: PDAC, lane 5: ADM, lane 6: AFL, lane 7: mouse tail. The recombined *kras*^{G12D} allele was present -as expected- only in the pancreatic tissues (lanes 3-6).

Supporting information

Figure S3

Example of *Kras*-mutated ADM-area with atypical flat lesions detected in one patient who underwent prophylactic total pancreatectomy due to a strong family history of pancreatic cancer. In this case a G→C point mutation was detected in codon 12.

Figure 1

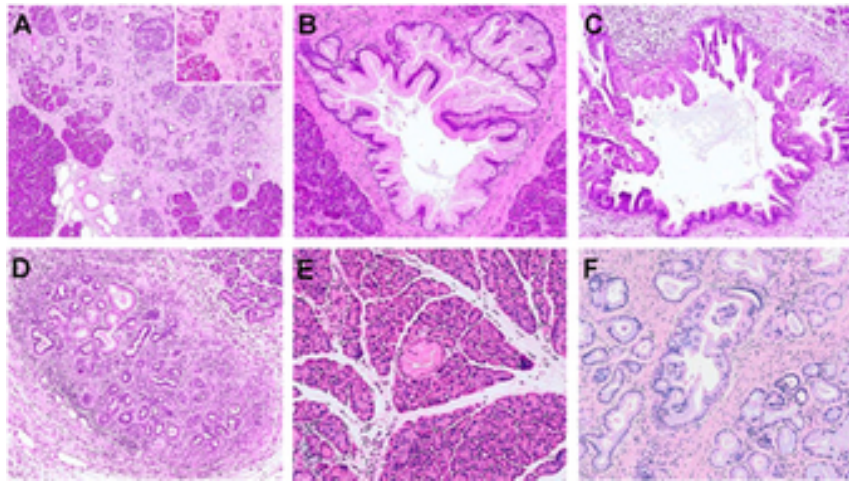


Figure 2

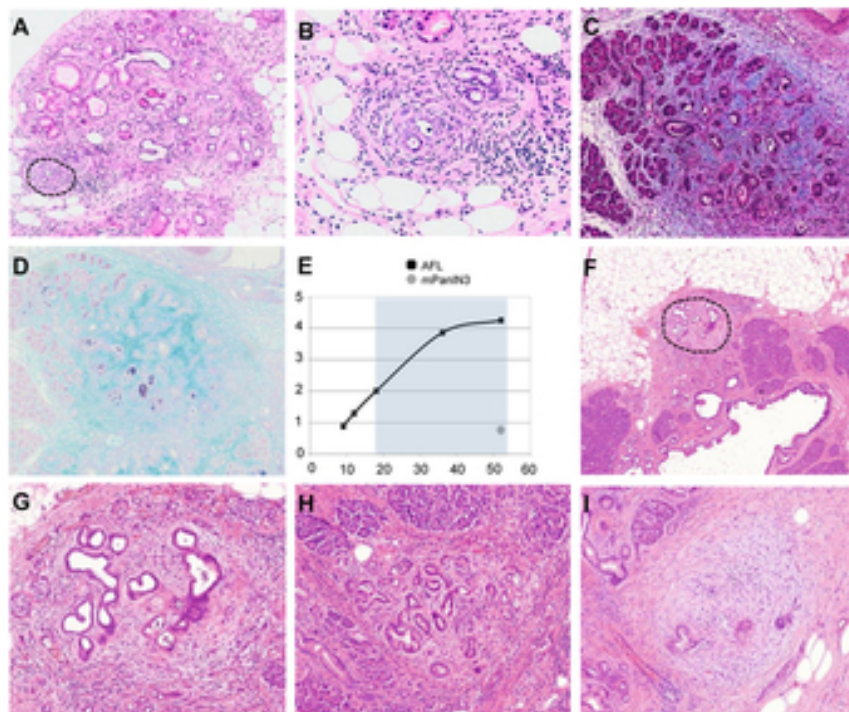


Figure 3

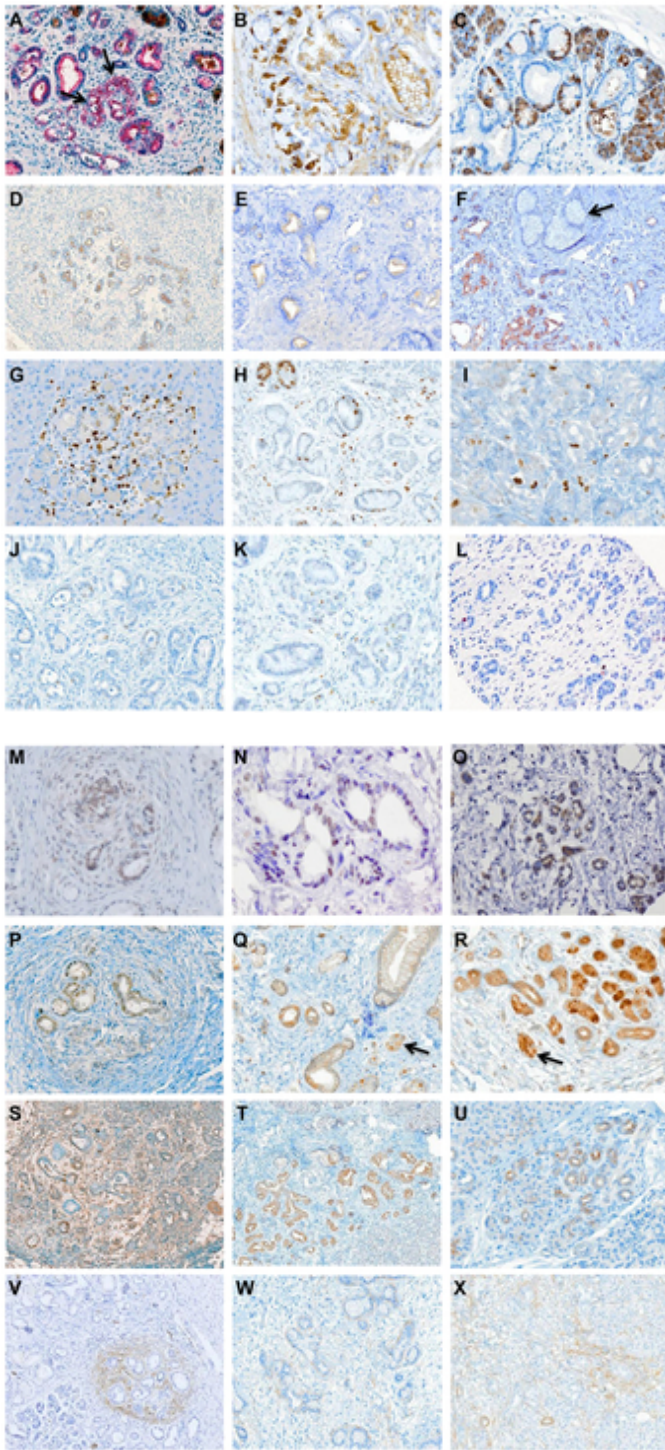


Figure 4

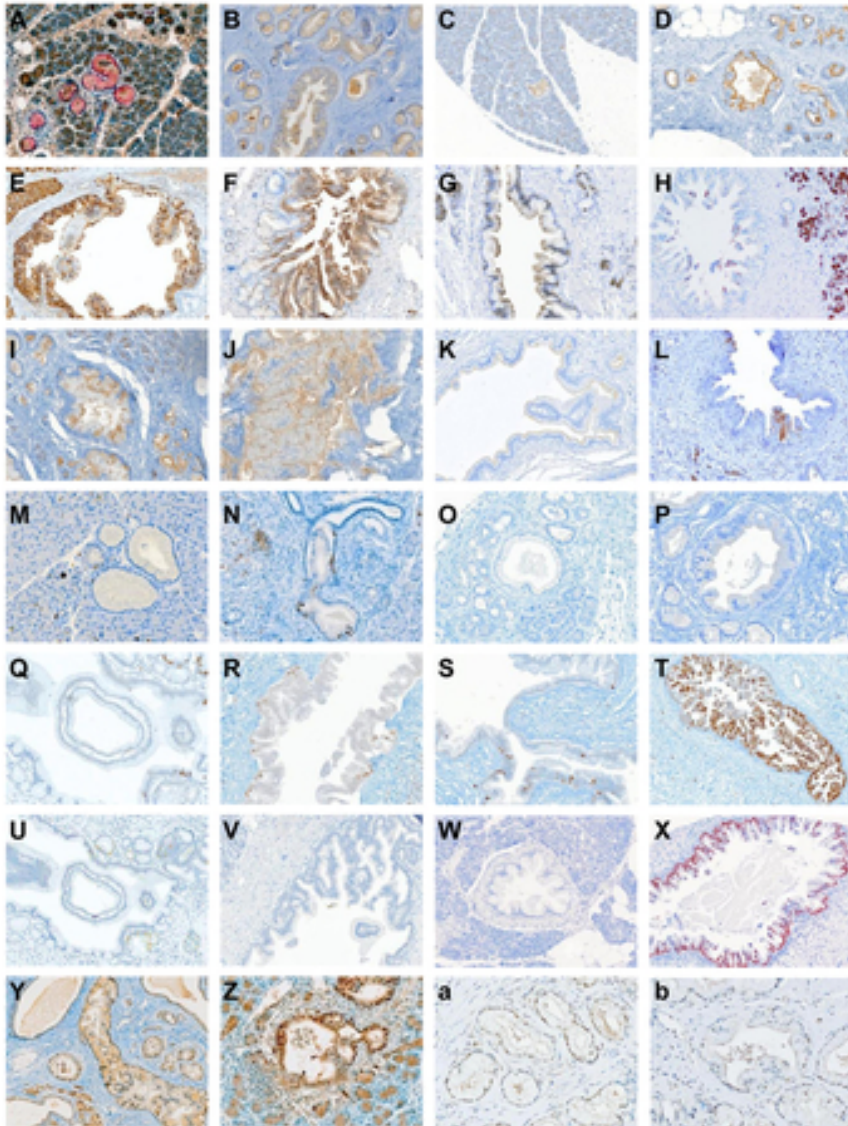


Figure 5

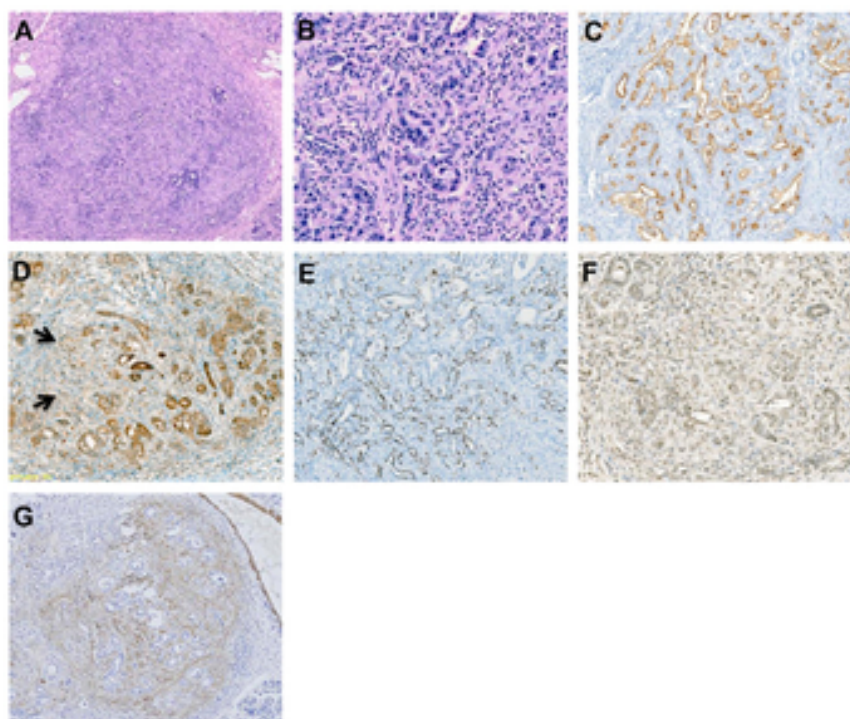


Figure 6

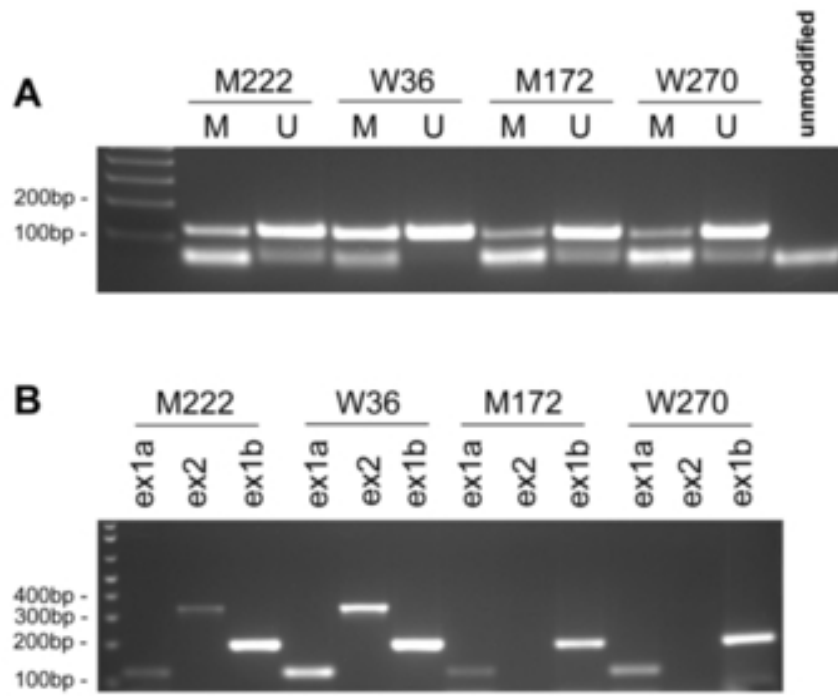
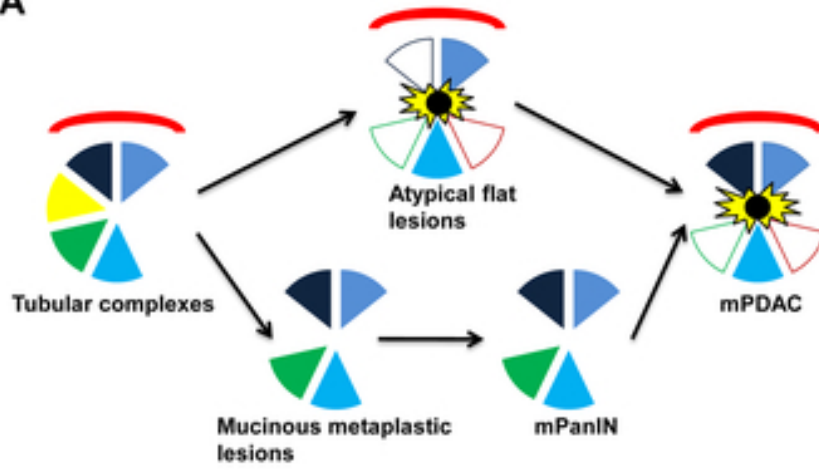


Figure 7

A



B

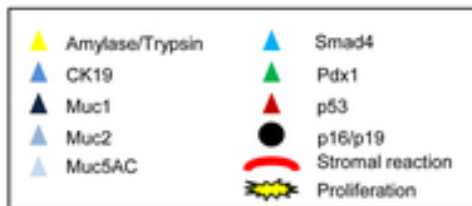
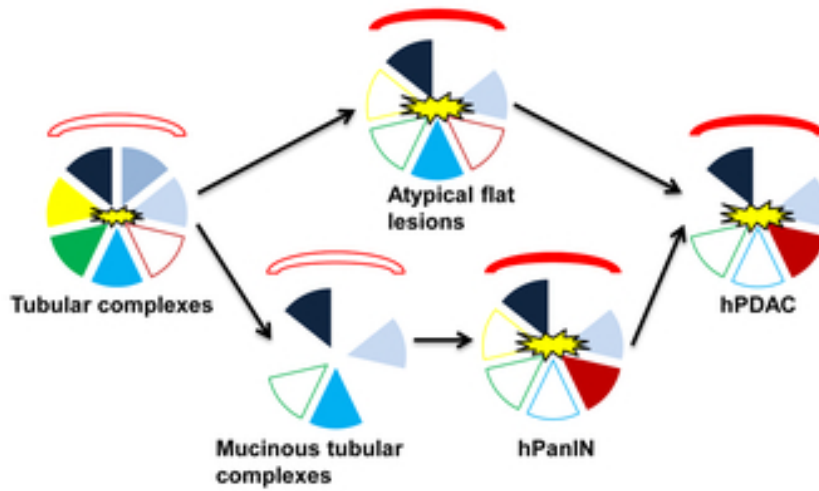


Figure S1

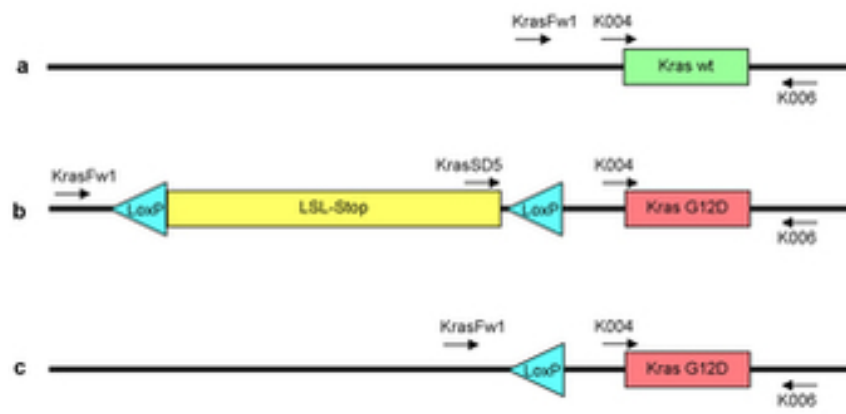


Figure S2

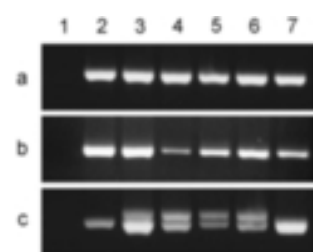


Figure S3

